JOURNAL OF BACTERIOLOGY, June 2006, p. 3983–3994 Vol. 188, No. 11
0021-9193/06/$08.00+0 doi:10.1128/JB.00033-06

Crl Activates Transcription Initiation of RpoS-Regulated Genes Involved in the Multicellular Behavior of *Salmonella enterica* Serovar Typhimurium

Véronique Robbe-Saule,[1] Valentin Jaumouillé,[1]† Marie-Christine Prévost,[2] Stéphanie Guadagnini,[2] Christelle Talhouarne,[1] Hayette Mathout,[1] Annie Kolb,[1] and Françoise Norel[1]*

Unité des Régulations Transcriptionnelles, URA-CNRS 2172,[1] and Plateforme de Microscopie Electronique,[2] Institut Pasteur, 25 rue du Docteur Roux, 75724 Paris Cedex 15, France

Received 10 January 2006/Accepted 15 March 2006

In *Salmonella enterica* serovar Typhimurium, the stationary-phase sigma factor σ^S (RpoS) is required for virulence, stress resistance, biofilm formation, and development of the rdar morphotype. This morphotype is a multicellular behavior characterized by expression of the adhesive extracellular matrix components cellulose and curli fimbriae. The Crl protein of *Escherichia coli* interacts with σ^S and activates expression of σ^S-regulated genes, such as the *csgBAC* operon encoding the subunit of the curli proteins, by an unknown mechanism. Here, we showed using in vivo and in vitro experiments that the Crl protein of *Salmonella* serovar Typhimurium is required for development of a typical rdar morphotype and for maximal expression of the *csgD*, *csgB*, *adrA*, and *bcsA* genes, which are involved in curli and cellulose biosynthesis. In vitro transcription assays and potassium permanganate reactivity experiments with purified His_6-Crl showed that Crl directly activated σ^S-dependent transcription initiation at the *csgD* and *adrA* promoters. We observed no effect of Crl on σ^{70}-dependent transcription. Crl protein levels increased during the late exponential and stationary growth phases in Luria-Beratani medium without NaCl at 28°C. We obtained complementation of the *crl* mutation by increasing σ^S levels. This suggests that Crl has a major physiological impact at low concentrations of σ^S.

Bacteria are routinely exposed to limited nutrients and other stressful conditions in their natural habitats. Consequently, they often grow and divide slowly and enter a stationary phase. The stationary-phase physiology, particularly multiple-stress resistance, and even cell morphology are determined by the general stress response. This response is controlled at the molecular level by a sigma subunit of RNA polymerase, σ^S (RpoS). In enterobacteria, RNA polymerase is composed of a core enzyme, E, with the subunit structure $\alpha_2\beta\beta'\omega$, which associates with one of the seven different σ subunits to form the holoenzyme ($E\sigma$). Each σ subunit targets the RNA polymerase to a different set of promoters, modulating the gene expression patterns. The RNA polymerase holoenzyme containing the σ^{70} subunit is responsible for the transcription of most genes during exponential growth. When an organism enters the stationary phase or when it is under specific stress conditions during the exponential growth phase (high osmolarity, low pH, or high and low temperatures), σ^S, which is encoded by the *rpoS* gene, accumulates in the cell, associates with the core enzyme, and directs the transcription of genes essential for the general stress response and for stationary-phase survival (for reviews see references 19 and 21). Regulation of σ^S occurs during transcription and posttranscription and involves numerous regulators (for a review see reference 19). Recent studies have shown that the *crl* gene product is a regulator of σ^S activity in *Escherichia coli* (8, 35). Crl modulates the expression of σ^S-regulated genes (*poxB*, *katE*, *bolA*, and *csgB*) (35). Crl also interacts directly with the σ^S protein in vitro and associates with $E\sigma^S$ at the *csgBAC* promoter, which governs the synthesis of curli fimbria subunits (8). However, the stimulating effect of Crl could not be reproduced in vitro with purified products, and the mechanism by which Crl influences σ^S activity is unknown.

To investigate the role of Crl at the molecular and physiological levels, our strategy was to first search for a particular phenotype associated with the *crl* knockout mutant. The Crl protein was initially implicated in the production of curli fibers in *E. coli* (1, 31, 32). These thin aggregative surface fimbriae, which are conserved among *Enterobacteriaceae*, are involved in a number of different processes. These processes include adhesion to soluble extracellular matrices, biofilm formation, interaction with eukaryotic cells, contact with major histocompatibility complex class I molecules, and induction of a proinflammatory response (2–7, 11, 14, 17, 20, 24, 31–33, 36, 42, 46, 47, 51, 54–57). Curli fimbriae and cellulose are the major components of the extracellular matrix involved in the multicellular behavior of *Salmonella* and some natural isolates of *E. coli* called the rdar (*r*ed *d*ry *a*nd *r*ough) morphotype (for a review see reference 40). Cells expressing the rdar morphotype absorb the dye Congo red (CR) from the medium and turn dark red. They have a dry and rough surface and form irregularly shaped, flat colonies that spread on plates (40) (Fig. 1). The rdar colonies also absorb the fluorescent dye calcofluor, which binds cellulose (41, 52, 58) (Fig. 1).

Expression of the rdar morphotype in *Salmonella enterica* serovar Typhimurium has been extensively studied. This morphotype occurs during the stationary growth phase under cer-

* Corresponding author. Mailing address: Institut Pasteur, Unité des Régulations Transcriptionnelles, URA-CNRS 2172, 25 rue du Docteur Roux, 75724 Paris Cedex 15, France. Phone: 33 140613122. Fax: 33 145688960. E-mail: francoise.norel@pasteur.fr.

† Present address: Unité de Pathogénie Microbienne Institut Pasteur, 28 rue du Docteur Roux, 75724 Paris Cedex 15, France.

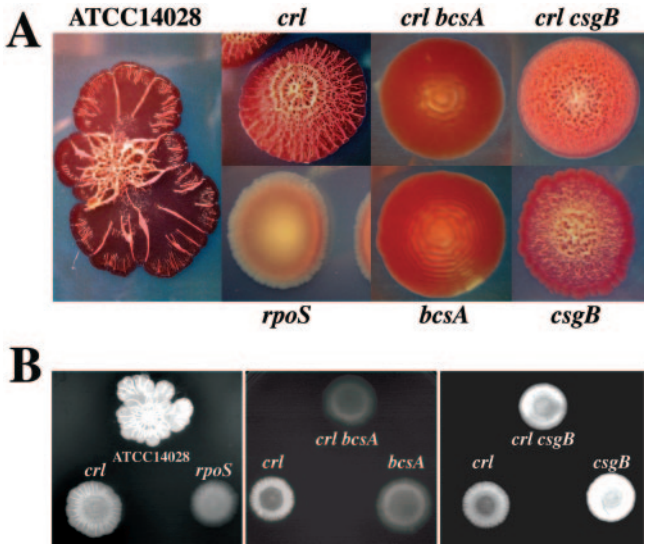

FIG. 1. rdar morphotypes of *Salmonella* strains: differential expression of the rdar morphotypes of *Salmonella* wild-type strain ATCC 14028 and its mutant derivatives ATCC*crl*, ATCC*rpoS*, ATCC*bcsA*, ATCC*csgB*, ATCC*crl bcsA*, and ATCC*crl csgB* after 5 days of growth at 28°C on CR plates (A) and on LB0 plates supplemented with calcofluor (B). ATCC 14028 and ATCC*rpoS* have typical rdar and saw morphotypes, respectively (42, 46). The *crl* mutant has a previously undescribed morphotype ($rdar_{crl}$), which was affected by elimination of curli production in the *crl csgB* double-mutant strain and by elimination of cellulose production in the *crl bcsA* double-mutant strain.

tain environmental conditions (for reviews see references 16 and 30) and is most efficient at low temperatures and low osmolarity. The rdar morphotype is positively regulated by *csgD*, a gene encoding a putative response regulator belonging to the FixJ family (for a review see reference 16). CsgD is required for expression of *csgBAC*, the operon encoding the curli subunits. CsgD also stimulates cellulose production via activation of transcription of *adrA*, which encodes a diguanylate cyclase protein (40, 52, 58). RpoS is required for development of the rdar morphotype and for *csgBAC*, *csgDEFG*, and *adrA* gene expression, although it is not known whether RpoS acts directly or indirectly at these promoters through CsgD or additional regulatory proteins (18, 31, 42, 45, 46, 52, 58).

Our studies indicated that expression of the rdar morphotype and transcription of the genes involved in curli and cellulose biosynthesis are affected in a *crl* knockout mutant of *Salmonella* serovar Typhimurium. In vitro transcription experiments with purified Crl protein of *Salmonella* showed that Crl stimulates σ^S-dependent transcription at the *adrA* and *csgD* promoters. This is the first report showing that Crl has a direct role in transcription initiation and that a *crl* knockout mutation has a physiological effect in *Salmonella*.

MATERIALS AND METHODS

Bacterial strains, phages, and growth conditions. The *E. coli* and *Salmonella* serovar Typhimurium strains used in this study are listed in Table 1. Bacteriophage P22HT105/1*int* was used to transduce mutations between *Salmonella* strains (49). Green plates, which were used to screen for P22-infected cells or lysogens, were prepared as described previously (53). Strains were routinely cultured at 37°C in Luria-Bertani (LB) medium unless indicated otherwise (48). Antibiotics were used at the following concentrations: carbenicillin, 100 μg ml^{-1}; chloramphenicol, 15 μg ml^{-1} for the chromosomal resistance gene and 30 μg ml^{-1} for the plasmid resistance gene; kanamycin, 50 μg ml^{-1}; and tetracycline, 20 μg ml^{-1}.

Phenotypic assays. For routine monitoring of multicellular behavior, *Salmonella* strains were grown on LB agar plates without NaCl (LB0) at 28°C. We determined colony morphology and color using LB0 agar supplemented with Congo red (40 μg ml^{-1}) and Coomassie brilliant blue (20 μg ml^{-1}) (CR plates), as described previously (41). We determined cellulose production using LB0 agar supplemented with calcofluor (fluorescent brightener 28; 50 μg ml^{-1}), as described previously (41). We detected calcofluor binding of agar-grown colonies by observing the cells under a 312-nm UV light source.

DNA manipulations. We used standard molecular biology techniques (39, 48) for DNA manipulations. DNA was sequenced by Genomexpress (Paris, France). Oligonucleotides were obtained from Distribio (France). Strains were constructed either by generalized transduction using phage P22HT105/1*int* (49) or by linear DNA transformation as described below.

Construction of plasmids. The plasmids used in this study are listed in Table 1. We determined the nucleotide sequence of a PCR-amplified *crl* gene from *Salmonella* strain ATCC 14028. The *crl* gene in ATCC 14028 was identical to that in *Salmonella* strain LT2 (http://genomeold.wustl.edu/projects/bacterial/styphimurium/). We constructed pAC*crl*-1 and pAC*crl*-2 by using primers specific for the ends of *crl* (5′-TTCCGAGAATTCTTATGCCGACAGTTTTACC GGCTCG-3′ and 5′-AGGCTCGAATTCTAAAGGAGATCGCAATGACGTT ACCGA-3′) to amplify a 0.5-kb promoterless *crl* gene from ATCC 14028 total DNA by PCR. EcoRI restriction sites (underlined) were incorporated at the 5′ and 3′ ends. After digestion with EcoRI, the fragment was inserted into the EcoRI site of pACYC184 in both orientations to obtain pAC*crl*-1 and pAC*crl*-2 (in pAC*crl*-1 the *crl* and *cat* genes are in the same orientation and the *crl* gene is likely transcribed from the *cat* promoter). We checked the nucleotide sequence of the *crl* insert in pAC*crl*-1 and pAC*crl*-2 by DNA sequencing. We constructed pQE*crl*, which expresses an N-terminal His_6 fusion to the *crl* gene product under the control of the pQE30 isopropyl-β-D-thiogalactopyranoside (IPTG)-inducible promoter, as follows. We used primers specific for the ends of *crl* (5′-AGGCT CGGATCCATGACGTTACCGAGTGGACACCCGA-3′ and 5′-TTCCGAAA GCTTTTATGCCGACAGTTTTACCGGCTCG-3′) to amplify a 0.45-kb fragment of ATCC 14028 total DNA by PCR. BamHI and HindIII restriction sites (underlined) were incorporated at the 5′ and 3′ ends, respectively. After digestion with BamHI and HindIII, the PCR-amplified fragment was ligated into the BamHI and HindIII sites of pQE30. We checked the nucleotide sequence of the *crl* insert in pQE*crl* by DNA sequencing. The DNA templates for in vitro transcription were prepared as follows. A 679-bp *csgD* fragment and a 172-bp *adrA* fragment were amplified by PCR from strain ATCC 14028 using primers 5′-GGGCTGCAGCACATCTGACAGCTGCCCCC and 5′-GGAGGATCCAG ATCATAATTTGTCG-3′ for *csgD* and primers 5′-CGAGAATTCGGCGTAG TGCTATCGG-3′ and 5′-GGCGGATCCGCCTGTTCAACCGC-3′ for *adrA*. After digestion with BamHI and PstI (underlined sites), the *csgD* promoter fragment from bp −684 to 121 relative to the transcriptional start site was inserted into BamHI- and PstI-digested pJCD01. The resulting plasmid was sequenced and designated pU-2750. After digestion with EcoRI and BamHI, the *adrA* promoter fragment from about bp −92 to 73 relative to the major transcriptional start site determined by using the homologous gene *yaiC* in *E. coli* (9) was inserted into EcoRI- and BamHI-digested pJCD01 to obtain pJCD*adrA*.

One-step inactivation of chromosomal genes and construction of chromosomal *lac* fusions. We created chromosomal mutations in the *rpoS*, *crl*, *csgB*, and *csgD* genes of *Salmonella* strain ATCC 14028 using PCR-generated linear DNA fragments and the λRed recombination method, as described by Datsenko and Wanner (13). Briefly, we used 63- to 66-nucleotide (nt) primers with 43- to 46-nt homology with the gene of interest on the 5′ end of the primer and 20-nt homology with the FLP recognition target-flanked antibiotic resistance cassette of plasmid pKD3 at the 3′ end (for sequences see reference 13). We used primers RpoS-P1 and RpoS-P2 (Table 2) for disruption of the *rpoS* gene, primers Crl-P1 and Crl-P2 for disruption of the *crl* gene, primers CsgB-P1 and CsgB-P2 for disruption of the *csgB* gene, and primers CsgD-P1 and CsgD-P2 for disruption of the *csgD* gene. ATCC 14028 containing plasmid pKD46, which carries the λ recombination genes *gam*, *bet*, and *exo* under control of the *araBAD* promoter (13), was grown overnight at 30°C, diluted in LB medium containing carbenicillin and L-arabinose (1 mM), and then grown to an optical density at 600 nm of 0.5. Electrocompetent cells were prepared, transformed with the PCR-generated linear fragments, plated on LB medium containing chloramphenicol (15 μg ml^{-1}), and incubated at 37°C. We then characterized the resulting colonies using a combination of PCRs performed with locus-specific primers and common test primers (13). Finally, isogenic strains were constructed by P22HT/*int*-mediated transduction of mutations into the appropriate strains. When required, the Cm^r resistance cassette was eliminated using temperature-sensitive helper plasmid

TABLE 1. Bacterial strains and plasmids used in this study

Strain or plasmid	Characteristics	Reference or source
E. coli strains		
JM109	*recA1 supE44 endA1 hsdR17 gyrA96 relA1 thi* Δ(*lac-proAB*) F′ (*traD36 proAB*$^+$ *lacI*^{q} *lacZ*Δ*M15*)	48
MC1061	*hsdR mcrB araD139* Δ(*araABC-leu*)*7679* Δ*lacX74 galU galK rpsL thi*	48
Salmonella serovar Typhimurium strains		
ATCC 14028	Wild type	American Type Culture Collection
ATCC*rpoS*	ATCC 14028 Δ*rpoS*::*cm*	This study
ATCC*crl*	ATCC 14028 Δ*crl*::*cm*	This study
ATCC*csgD*	ATCC 14028 Δ*csgD*::*cm*	This study
ATCC*csgB*	ATCC 14028 Δ*csgB*::*cm*	This study
ADR1a	MAE52 *adrA*::MudJ	45
MAE150	MAE52 *bcsA*::MudJ	58
ATCC*adrA*	ATCC 14028 *adrA*::MudJ	This study
ATCC*bcsA*	ATCC 14028 *bcsA*::MudJ	This study
ATCC*rpoScrl*	ATCC 14028 Δ*rpoS* Δ*crl*::*cm*	This study
ATCC*csgB-lacZ*	ATCC 14028 *csgB-lacZY*	This study
ATCC*csgD-lacZ*	ATCC 14028 *csgD-lacZY*	This study
ATCC*rpoScsgD*	ATCC 14028 Δ*rpoS* Δ*csgD*::*cm*	This study
ATCC*rpoSbcsA*	ATCC 14028 Δ*rpoS*::*cm bcsA*::*MudJ*	This study
ATCC*rpoSadrA*	ATCC 14028 Δ*rpoS*::*cm adrA*::*MudJ*	This study
ATCC*rpoScsgD-lacZ*	ATCC 14028 Δ*rpoS*::*cm csgD-lacZY*	This study
ATCC*rpoScsgB-lacZ*	ATCC 14028 Δ*rpoS*::*cm csgB-lacZY*	This study
ATCC*crlbcsA*	ATCC 14028 Δ*crl*::*cm bcsA*::*MudJ*	This study
ATCC*crlcsgB*	ATCC 14028 Δ*crl* Δ*csgB*::*cm*	This study
ATCC*crladrA*	ATCC 14028 Δ*crl*::*cm adrA*::*MudJ*	This study
ATCC*crlcsgD-lacZ*	ATCC 14028 Δ*crl*::*cm csgD-lacZY*	This study
ATCC*crlcsgB-lacZ*	ATCC 14028 Δ*crl*::*cm csgB-lacZY*	This study
ATCC*csgDadrA*	ATCC 14028 Δ*csgD*::*cm adrA*::*MudJ*	This study
ATCC*csgDbcsA*	ATCC 14028 Δ*csgD*::*cm bcsA*::*MudJ*	This study
ATCC*csgDcsgB-lacZ*	ATCC 14028 Δ*csgD*::*cm csgB-lacZY*	This study
Plasmids		
pQE30	Cb^r, for expression of His-tagged proteins	QIAGEN
pQE*crl*	Cb^r, pQE30::*crl*, expresses a His_6-Crl protein	This study
pACYC184	Cm^r Tet^r, cloning vector	10
pAC*crl*-1	Tet^r, pACYC184::*crl*, *cat*, and *crl* in the same orientation	This study
pAC*crl*-2	Tet^r, pACYC184::*crl*, *cat*, and *crl* in the opposite orientation	This study
pSTK4	Cm^r, pACYC184::*rpoS*	23
pJCD01	Cb^r, pUC with transcriptional terminators	28
pJCD*adrA*	Cb^r, pJCD01::*adrA*	This study
pGO1	Cb^r, pJCD01::*lac*	34
pU-2750	Cb^r, pJCD01::*csgD*	U. Gerstel et al., unpublished

pCP20, which encodes the FLP recombinase (13). We constructed single-copy *csgB-lacZY* and *csgD-lacZY* transcriptional gene fusions from mutants ATCC*csgB*::Cm and ATCC*csgD*::Cm using conditional plasmids containing promoterless *lacZY* genes and the FLP recognition target site, as described previously (15). We then used PCR assays to ensure that the plasmids were integrated in the correct location and to determine the presence of multiple plasmid integrants (using common test primers, such as those described by Ellermeier et al. [15]). We also used flanking locus-specific primers to amplify junction fragments that were subsequently analyzed by DNA sequencing. Isogenic strains were constructed by P22HT/*int*-mediated transduction of the mutations into the appropriate strains.

TABLE 2. Primers used for gene mutagenesis

Primer	Sequence	Gene mutated
RpoS-P1	GTCAGAATACGCTGAAAGTTCATGATTTAAATGAAGACGCGGAGTGTAGGCTGGAGCTGCTTC	*rpoS*
RpoS-P2	CTCGCGGAACAGCGCTTCGATATTCAGCCCCTGCGTCTGCAGACATATGAATATCCTCCTTAG	*rpoS*
Crl-P1	CAGTTGCTTCATTAAAGGAGATCGCAATGACGTTACCGAGTGGGTGTAGGCTGGAGCTGCTTC	*crl*
Crl-P2	CTGATGGCGCTGCGCCATCAGGCATGGCAGCAGGGTTATGCCGCATATGAATATCCTCCTTAG	*crl*
CsgB-P1	GATAATTTTCGCTATGTACGACCAGGTCCAGGGTGACAGCATGAAAGTGTAGGCTGGAGCTGCTTC	*csgB*
CsgB-P2	CCCATCGGATTGATTTAAAAGTCGTAACGGTATTAGCGTTGGGTGCATATGAATATCCTCCTTAG	*csgB*
CsgD-P1	GCTGTCAGATGTGCGATTAAAAAAAGTGGAGTTTCATCATGTTGTGTAGGCTGGAGCTGCTTC	*csgD*
CsgD-P2	GCTGCTACAATCCAGGTCAGATAGCGTTTCATGGCCTTACCGCCATATGAATATCCTCCTTAG	*csgD*

Antibodies, electrophoresis, and immunoblot analysis of proteins. Preparation of whole-cell extracts and sodium dodecyl sulfate (SDS)-polyacrylamide gel electrophoresis were carried out as described by Silhavy et al. (50). We determined the amounts of protein in whole-cell lysates using a DC protein assay kit (Bio-Rad). We loaded equal amounts of protein in each slot. The relative molecular weights of the proteins were estimated using molecular weight standards (Euromedex). Denaturing SDS-polyacrylamide gels were stained using Bio-Safe Coomassie blue (Bio-Rad). Antibodies against the Crl protein of *Salmonella* were produced in rabbits by injecting highly purified His_6-Crl protein (P.A.R.I.S Production d'Anticorps, France). Rabbit antibodies against the σ^S protein of *S. enterica* serovar Typhimurium were obtained from Coynault et al. (12). Proteins were transferred on Hybond P membranes (Amersham Life Sciences) and incubated with the polyclonal rabbit antibody serum as previously described (12). The bound antibodies were detected using a secondary anti-rabbit antibody linked to peroxidase and an ECL Plus Western blot detection system kit (Amersham Life Sciences).

Electron microscopy. Electron microscopy was performed with bacteria that had been grown for 5 to 6 days on LB0 plates at 28°C. For scanning electron microscopy, bacteria were fixed in 2.5% (vol/vol) glutaraldehyde in 0.1 M cacodylate buffer (pH 7.2) by incubation for 1 h at room temperature. They were then washed three times for 5 min each time in 0.2 M cacodylate buffer (pH 7.2), postfixed by incubation for 1 h in 1% (wt/vol) osmium tetroxide in 0.2 M cacodylate buffer (pH 7.2), and then rinsed with distilled water. Bacteria were dehydrated by incubation in a graded series of 25, 50, 75, and 95% ethanol solutions for 5 min for each solution. Samples were then dehydrated by incubation for 10 min in 100% ethanol, followed by critical point drying with CO_2. Dried specimens were sputter coated with 15 nm of gold-palladium, using a GATAN ion beam coater. Cells were then examined with a JEOL JSM 6700F field emission scanning electron microscope operating at 5 kV, using secondary electron detectors. For transmission electron microscopy, agar pieces containing bacteria were cut, fixed, treated with ruthenium red (25), and embedded in SPURR resin. We used ruthenium red dye for staining bacterial polysaccharide. We avoided disturbing the fragile extracellular material by fixing and staining the bacteria directly on agar, followed by analysis of thin sections. The fixation and processing steps were carried out in a fume cupboard at room temperature in vials on a rotary mixer. Bacteria were fixed by incubation for 2 h in 3% glutaraldehyde containing 0.75% ruthenium red in 0.1 M sodium cacodylate buffer (pH 7.4). The samples were then washed four times in 0.2 M sucrose–0.075 M sodium cacodylate buffer (pH 7.4) by incubation for 90 min and postfixed with 1% osmium tetroxide–0.75% ruthenium red in cacodylate buffer (pH 7.5). Samples were then washed twice in ultrapure water and three times in 0.1 M cacodylate buffer (pH 7.4). Samples were subsequently dehydrated by incubation in a graded series of 30 to 100% ethanol solutions for 15 min per step, followed by incubation for 90 min in pure ethanol and for 15 min in propylene oxide. The samples were then sequentially transferred into 3:1, 1:1, 1:3 propylene oxide—low-vicosity Agar Resin LV (Agar Scientific, Oxford Instrument, France) by incubation for 1 h per step. They were finally incubated in 100% resin overnight. The samples were incubated in fresh resin three times for 3 h, embedded in silicone flat molds, and polymerized by incubation at 60°C for 2 days. Ultrathin transverse sections were cut using a diamond knife and a Leica Ultracut UCT (Leica Microsystems SA, Rueil Malmaison, France). The grid-mounted sections were stained with uranyl acetate and lead citrate. Electron micrographs were recorded using a Mega view charge-coupled device camera (ELOISE SARL, France) mounted on a JEOL 1200 EX II transmission electron microscope (JEOL EUROPE SA) operating at 80 kV.

Enzymatic assay. β-Galactosidase activity was measured as described by Miller (29) and was expressed in Miller units.

Overproduction and purification of His_6-Crl. A 4-liter culture of JM109 carrying pQE*crl* was grown in LB medium containing 100 μg ml^{-1} ticarpen at 37°C to an optical density of 0.6, and then 1 mM IPTG was added. The cells were harvested after 4 h, washed, resuspended in 60 ml of buffer A (50 mM Na_2HPO_4 [pH 8], 300 mM NaCl) supplemented with 1 mM 4-(2-aminoethyl)-benzenesulfonyl fluoride, and then lysed by sonication. The crude cell extract was centrifuged at 15,000 × *g* for 30 min. The supernatant was added to 10 ml of Ni-nitrilotriacetic acid agarose (QIAGEN) and gently mixed for 1 h. The slurry was packed onto an Econo-Pac column (Bio-Rad) and washed with 250 ml of buffer A containing 20 mM imidazole. His_6-Crl was eluted with buffer A containing 250 mM imidazole, dialyzed against buffer B (20 mM Tris-HCl [pH 8], 20 mM NaCl), and loaded onto a Hitrap Q anion-exchange column (5 ml; GE Healthcare). After washing with 10 ml of buffer B, His_6-Crl was eluted from the column between 0.4 M and 0.6 M NaCl using a linear 0.02 to 1 M NaCl gradient. We pooled only the first fractions, which were dialyzed against buffer C (10 mM Tris-HCl [pH 8], 10 mM $MgCl_2$, 100 mM KCl, 50% glycerol, 1 mM dithiothreitol [DTT]). This resulted in 14 mg of purified His_6-Crl, as determined by the Bradford assay.

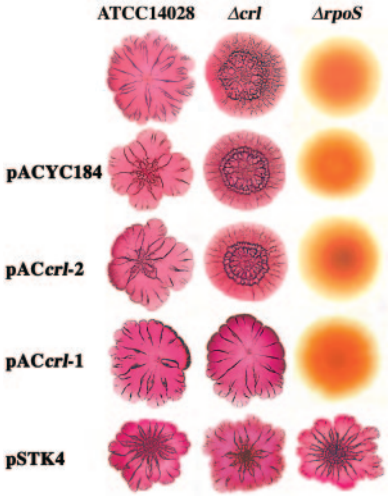

FIG. 2. rdar morphotypes of *Salmonella* strains harboring different plasmids, including ATCC 14028 and Δ*crl* and Δ*rpoS* mutant derivatives of this strain that harbor the vector pACYC184, the *crl* gene on pAC*crl*-1 and pAC*crl*-2, and the *rpoS* gene on pSTK4 (Table 1), after 5 days of growth on CR plates at 28°C. In pAC*crl*-2 the *crl* gene was cloned in the promoterless orientation. Complementation of the *crl* mutation was observed with pAC*crl*-1 and pSTK4. Complementation of the *rpoS* mutation was observed with pSTK4.

Runoff transcription assays. Single-round transcription assays were performed by using pU-2750 and pJCD*adrA* digested with the AseI restriction enzyme. The 285-bp *lac*UV5 fragment was synthesized by PCR using primer E5 (5′-CCTGG CAGTTCCCTACTCT-3′) and primer E7 (5′-CTGGCAGATGCGTCTTCCG-3′) with the pGO1 plasmid (34). Reconstituted RNA polymerase (60 nM) (σ/core ratio, 2.5: 1) was incubated in buffer T (40 mM HEPES [pH 8.0], 10 mM $MgCl_2$, 100 mM potassium glutamate, 2 mM DTT) with different concentrations of Crl (0, 0.5, 2, and 8 μM) for 20 min at 30°C. DNA templates were added at a final concentration of 10 nM, and the mixtures were incubated for 12 min at 30°C. Elongation was started by adding 3 μl of a mixture containing 1 mM ATP, 1 mM GTP, 1 mM CTP, 100 μM UTP, 0.5 μCi [α-^{32}P]UTP, and 600 μg ml^{-1} heparin to the template polymerase mixture. After 10 min, the reactions were stopped by adding formamide containing 10 mM EDTA, xylene cyanol, bromophenol blue, and 1% SDS. After heating to 90°C, the samples were subjected to electrophoresis on a 7.5% polyacrylamide sequencing gel, and the transcripts were quantified using a PhosphorImager (Molecular Dynamics). The transcript sizes were approximately 191 nt for the *csgD* promoter, 158 nt for the *adrA* promoter, and 128 nt for the *lac*UV5 promoter.

Abortive initiation assays. We used the 172-bp *adrA* fragment described above and the 191-bp *csgD* fragment (synthesized by PCR using primers 5′-CTGTGG GTTGAAATAGCCCATTATCC-3′ and 5′-CCCGGATCCCAACTTTACTAT CAAATCTAAAC-3′) as templates with the dinucleotide initiators ApA for *adrA* and ApG for *csgD* to synthesize ApApUpU and ApGpUpU, respectively. ApApUpU is complementary to the *adrA* template strand located between nt 8 and 11 downstream from the last T of the Pribnow box. This transcription start site maps close to that identified for the homologous *yaiC* gene in *E. coli* (9). A mixture of DNA template (10 nM), dinucleotide (1 mM), and 60 nM [α-^{32}P]UTP was added to an equal volume of the holoenzyme (60 nM) preincubated with buffer or Crl at various concentrations. In the case of the *lac*UV5 fragment the UTP concentration was 50 μM (27). Aliquots were removed at various times. The aliquots were spotted onto Whatmann 3MM paper prespotted with 100 mM EDTA, and chromatograms were developed as previously described (27).

$KMnO_4$ reactivity experiments. We generated the 172-bp *adrA* and 191-bp *csgD* fragments by PCR using a combination of an unlabeled primer and a primer end labeled with T4 polynucleotide kinase and [γ-^{32}P]ATP. Open complexes were allowed to form in buffer T without DTT by incubation at 30°C for 20 min and were incubated with $KMnO_4$ (3 mM) for 15 s. The reaction was stopped by adding 3 μl of DTT (200 mM) and 200 μl of a solution containing 0.4 M sodium acetate (pH 8.0), 2.5 mM EDTA, and 60 μg ml^{-1} of salmon sperm DNA. After phenol extraction and precipitation with ethanol, the samples were resuspended in 100 μl of piperidine (1 M), heated at 90°C for 30 min, evaporated to dryness,

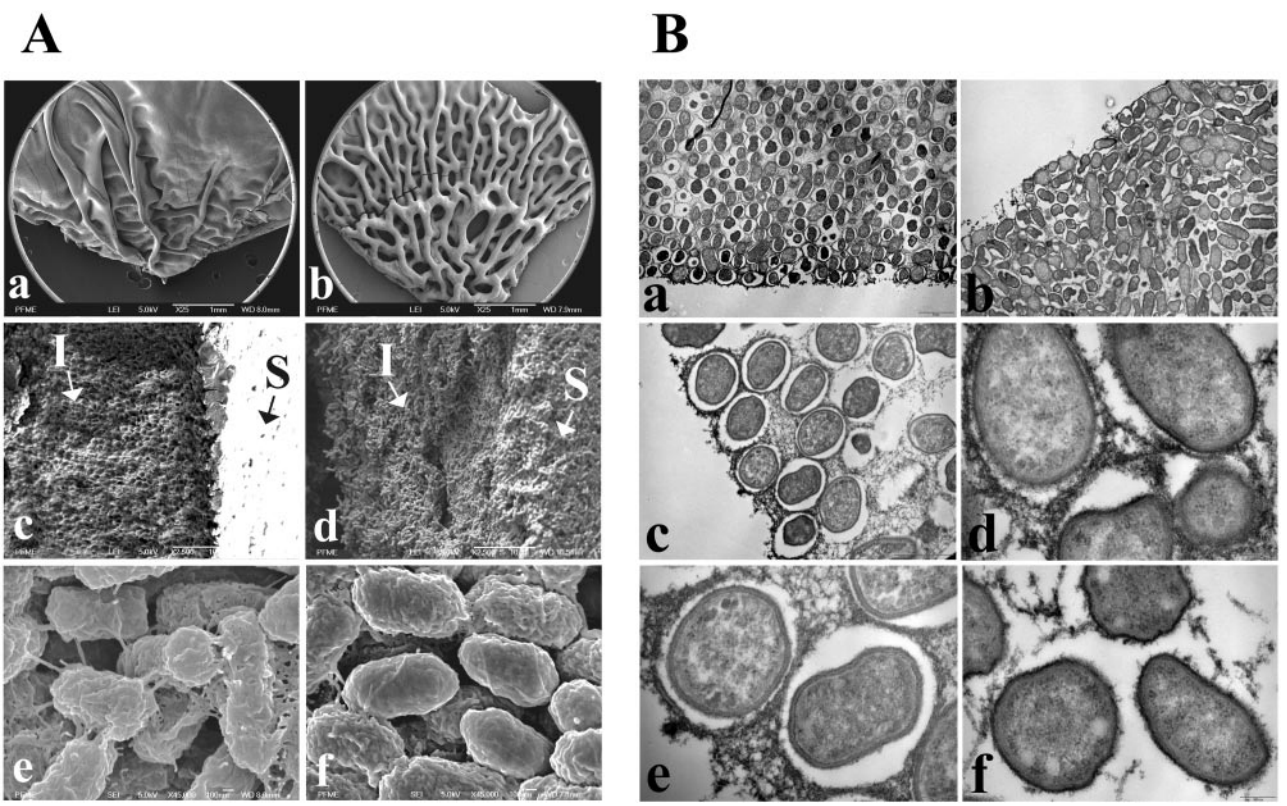

FIG. 3. Electron micrographs of colonies of *Salmonella* strains. (A) Scanning electron micrographs of wild-type strain ATCC 14028 (panels a, c, and e) and ATCC*crl* (b, d, and f) after 5 days of growth on CR plates at 28°C. Panels a and b show one-quarter of a colony (upper surface). Panels c and d show cross fractures of colonies, revealing the inner structure. The arrows indicate the surface (S) and the inner part (I) of the colony. In panel c, bacteria were extruded from the cross fracture, revealing the inner compartmentalization with a highly organized matrix having a honeycomb-like structure. Panels e and f show the upper, air-facing surfaces of colonies, revealing the extracellular matrix and cell-cell interactions. The magnifications are ×25 for panels a and b, ×2,500 for panels c and d, and ×45,000 for panels e and f. (B) Representative transmission electron micrographs of ruthenium red-stained transverse ultrathin sections of wild-type (panels a, c, and e) and *crl* (panels b, d, and f) colonies of *Salmonella* after 5 days of growth on LB0 at 28°C. The electron micrographs show the presence of closely packed bacteria and a stained matrix between cells. However, the biofilm formed by the wild-type strain was homogeneously stained, whereas the biofilm formed by the *crl* strain has a less well-organized structure, and areas have either an extensive extracellular matrix (panel d) or very little matrix (panel f). The magnifications are ×7,500 for panels a and b, ×25,000 for panel c, and ×75,000 for panels d, e, and f.

and evaporated twice with 20 μl water. The samples were resuspended in formamide containing 20 mM EDTA, bromophenol, and xylene cyanol blue and loaded onto an 8% denaturing polyacrylamide gel. The gels were dried and analyzed using a PhosphoImager.

RESULTS

rdar morphotype development is affected by a *crl* knockout mutation. We determined the role of *crl* in the rdar morphotype of *Salmonella* by plating ATCC 14028 and Δ*crl* and Δ*rpoS* mutant derivatives of this strain on LB0 plates containing either CR Fig. 1A) or calcofluor (Fig. 1B) and incubating the plates at 28°C. ATCC 14028 developed a typical rdar morphotype and bound CR and calcofluor (Fig. 1A and B). Curli and cellulose production requires RpoS. Therefore, the *rpoS* mutant did not bind the dyes and displayed a saw (*s*mooth *a*nd *w*hite) morphotype (42, 46, 52, 58) (Fig. 1A and B). The *crl* mutant developed a rough and dry morphotype and bound both CR and calcofluor (Fig. 1A and B). However, the *crl* colonies were organized differently than the wild type colonies ($rdar_{crl}$ morphotype). Introducing plasmid pAC*crl*-1 expressing the Crl protein into the *crl* mutant restored the typical rdar morphotype (Fig. 2), whereas we observed no complementation with the negative controls pACYC184 and pAC*crl*-2, in which the *crl* gene was cloned in the promoterless orientation (Fig. 2). Together, these results showed that expression of a typical rdar morphotype in *Salmonella* serovar Typhimurium required Crl.

***crl* mutant still produces curli and cellulose, but the architecture of the colonies is affected.** We determined whether curli and cellulose contribute to the specific morphotype ($rdar_{crl}$) of the *crl* mutant by introducing mutations into the biosynthetic curli (*csgB*) and cellulose (*bcsA*) genes in the *crl* mutant. We examined the morphotypes of the double mutants after 5 days of growth at 28°C on LB0 plates containing CR and calcofluor. The *bcsA* mutation eliminated calcofluor binding by the *crl* strain (Fig. 1B). Also, on CR plates, the *crl csgB* and *crl bcsA* strains had different morphotypes than the *crl* strain (Fig. 1A). These results showed that curli and cellulose production contributed to the $rdar_{crl}$ morphotype of the *crl* strain.

We investigated the architecture of the colonies of the wild-type and *crl* strains after 5 days of growth on LB0 at 28°C by microscopic analysis (Fig. 3). Scanning electron microscopy of colonies formed by the wild-type and *crl* strains revealed a

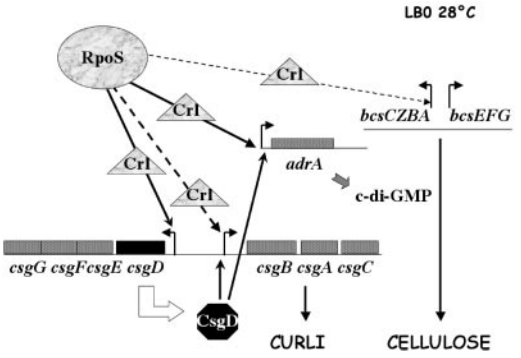

FIG. 4. Schematic representation of gene regulation controlling curli and cellulose expression in *Salmonella*. Positive regulation by RpoS, Crl, and CsgD is indicated by arrows. Solid lines indicate a direct role for RpoS and Crl in activating transcription initiation at the *adrA* and *csgD* promoters. Dashed lines indicate either a direct role or an indirect role for RpoS and Crl, and the thickness of the line indicates the strength of control. Positive regulation by CsgD is indicated by solid lines because putative CsgD binding sites have been found upstream from the *csgB* and *adrA* promoters (9). However, so far there is no evidence for CsgD binding. See text for details.

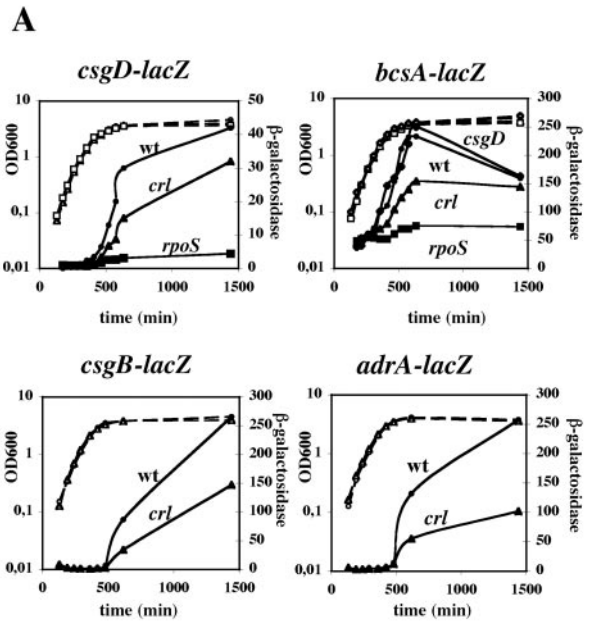

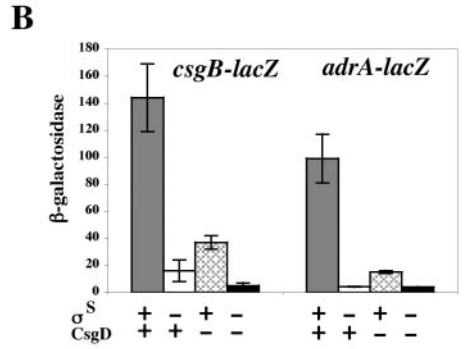

FIG. 5. Expression of curli and cellulose biosynthesis genes in *Salmonella* wild-type and mutant strains. (A) Expression of *csgD-lacZ*, *csgB-lacZ*, *adrA-lacZ*, and *bcsA-lacZ* gene fusions as a function of bacterial cell growth. Wild-type strain ATCC 14028 (wt) and the ATCC*crl*, ATCC*rpoS*, and ATCC*csgD* mutant strains harboring fusions were grown in LB0 at 28°C. Exponential-phase cultures (optical density at 600 nm [OD600], 0.5) of *Salmonella* were diluted in LB0 prewarmed at 28°C to prolong the exponential phase. Aliquots were removed at various times, and β-galactosidase activity was measured (solid symbols) by the method of Miller (29). The growth phase was determined by measuring the culture turbidity at an optical density of 600 nm (open symbols and dashed lines). The experiments were repeated twice, and the results of a representative experiment are shown. (B) Expression of *csgB-lacZ* and *adrA-lacZ* gene fusions in *Salmonella* wild-type and *rpoS*, *csgD*, and *rpoS csgD* mutant strains grown to the stationary phase (18 h of growth) in LB0 at 28°C.

bacterial pellicle that was several cell layers thick in both types of colonies (Fig. 3A, panels a to d). However, the *crl* colony architecture was different from the wild-type colony architecture. There were extensive folds of the bacterial *crl* pellicle (Fig. 3A, compare panels a and b). We observed cell-cell interactions and production of an extracellular matrix in both the wild-type and *crl* strains (Fig. 3A, panels e and f).

The extracellular matrix was analyzed further by transmission electron microscopy. Ultrathin sections were stained with ruthenium red, which preferentially stains polysaccharides, such as cellulose (25, 44, 52). In the wild-type colonies, an abundant ruthenium red-positive matrix between the bacteria was observed, whereas in the *crl* strain the matrix was less abundant and less well organized (Fig. 3B). In the mutant, the pattern was heterogeneous; there were areas of cells enclosed in a ruthenium red-stained matrix (Fig. 3B, panel d), and there were areas of cells with no matrix (Fig. 3B, panel f). The orientations of the cells themselves were also slightly different for the wild-type strain and the *crl* mutant. Matrix-enclosed wild-type cells were tightly packed and aligned in a honeycomb-like structure, whereas the *crl* cells appeared to be more randomly distributed (Fig. 3B, panels a, c, and b). We also observed this difference in the organization of the structure in scanning electron micrographs of cross fractures that showed the inner parts of colonies (Fig. 3A, panels c and d).

***crl* knockout mutation decreases curli and cellulose gene transcription.** RpoS and CsgD are known to positively regulate the production of the extracellular matrix components cellulose and curli (for reviews see references 16 and 40) (Fig. 4). Curli biogenesis requires two divergently transcribed operons, the *csgBAC* operon, encoding the structural components of curli, and the *csgDEFG* operon. Activation of the *csgBAC* operon and the *adrA* gene, which encodes a protein that mediates production of cyclic di-(3′,5′)-guanylate, requires CsgD. The genes involved in cellulose biosynthesis are organized into two divergently transcribed operons, *bcsABZC* and *bcsEFG*. The allosteric activator cyclic di-(3′,5′)-guanylate binds to the BcsB subunit of the cellulose synthase, stimulating cellulose biosynthesis. Expression of the *csg* operons and the *adrA* gene depends on *rpoS*.

To determine the role of *crl* in the expression of σ^S-regulated genes involved in the rdar morphotype, we constructed chromosomal *csgD-lacZ*, *csgB-lacZ*, and *adrA-lacZ* transcriptional fusions at the loci of the wild-type alleles. Expression of the fusions was monitored during growth of wild-type and *crl* strains (Fig. 5A). Cells were grown in LB0 at 28°C. This al-

lowed maximal expression of these genes (30, 45, 46). The expression of the *csgD*, *csgB*, and *adrA* genes was substantially reduced in the *crl* mutant compared to the expression in the wild-type strain (Fig. 5A). As expected, *csgD*, *csgB*, and *adrA* expression was considerably reduced in the *rpoS* mutant (Fig. 5A and B). The effect of the *rpoS* mutation on *csgB* and *adrA* expression was even more drastic than the effect on *csgD* expression (Fig. 5B). Expression of *csgB* and expression of *adrA* were decreased 10-fold and 20-fold, respectively, in the *rpoS* mutant and only 4-fold and 6-fold, respectively, in the *csgD* strain (Fig. 5B). We observed no detectable expression of these genes in the *csgD rpoS* double mutant (Fig. 5B).

The *bcs* genes are thought to be constitutively transcribed, and their expression is not dependent on CsgD, AdrA, and RpoS (58). Accordingly, we found that expression of a chromosomal *bcsA-lacZ* gene fusion was not decreased in the *csgD* mutant (Fig. 5A). However, the levels of expression of the *bcsA-lacZ* gene fusion in the *rpoS* and *crl* strains were lower than the levels of expression in the wild type after 10 h of growth (Fig. 5A). Nevertheless, the pattern of *bcsA* gene fusion expression was substantially different from the pattern of expression of the *adrA*, *csgB*, and *csgD* gene fusions, as follows: (i) *bcsA* was transcribed during the exponential growth phase, although its transcription increased in the stationary phase in a σ^S-dependent manner; (ii) the *rpoS* mutation affected *bcsA* gene expression much less than it affected *csgD*, *csgB*, and *adrA* gene expression, and the effect of the *rpoS* mutation on *bcsA* gene expression was maximal in the early stationary phase; and (iii) transcription of *bcsA* probably decreased during the late stationary growth phase.

Consistent with the typical rdar morphotype developed by the *crl* strain containing pAC*crl*-1 (Fig. 2), we observed complementation of the *crl* mutation by pAC*crl*-1 for *csgD*, *csgB*, *adrA*, and *bcsA* gene expression (data not shown). Together, these results demonstrated that Crl plays a role in the transcription activation of the *csgD*, *csgB*, *adrA*, and *bcsA* genes required for developing a typical rdar morphotype in *Salmonella*.

Crl protein levels increase in the late exponential and stationary growth phases. Using Western blotting, we examined expression of the Crl protein in cells grown in LB0 at 28°C (Fig. 6). In wild-type strain ATCC 14028, the Crl protein was synthesized during the early exponential growth phase, but Crl protein levels increased during the late exponential and stationary growth phases. This expression pattern is consistent with previous results showing that Crl increases the expression of genes involved in the rdar morphotype when cells enter the stationary phase. The expression pattern of the Crl protein did not seem to be affected in the *rpoS* strain under the environmental conditions used (Fig. 6). We determined whether the *crl* mutation affected *rpoS* expression in LB0 at 28°C by comparing the σ^S levels in the *crl* and wild-type strains (Fig. 6). Higher levels of σ^S were found in the *crl* mutant. This is consistent with previous results for *E. coli* which showed that RpoS production is increased by a *crl* mutation (8, 35). Thus, a higher level of σ^S in the *crl* strain seems to be less active for *csgD*, *csgB*, *adrA*, and *bcsA* gene expression than a lower level of σ^S in the wild-type strain.

Expression of *rpoS* from a plasmid can restore a typical rdar morphotype in the *crl* strain. The cloned *rpoS* gene on pSTK4

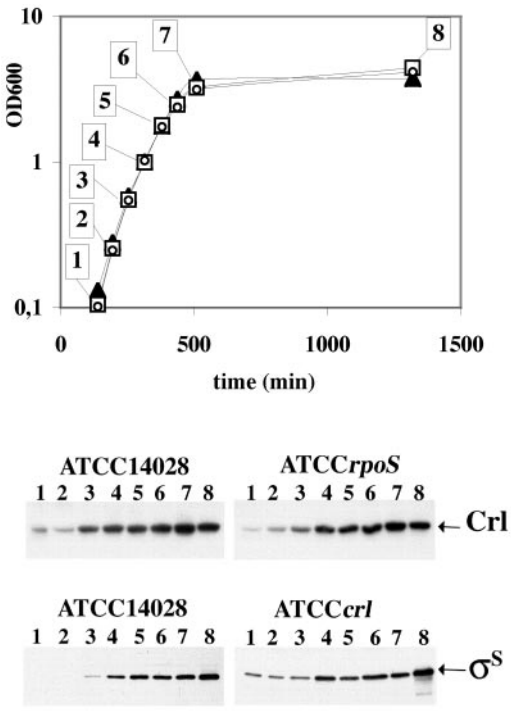

FIG. 6. Expression of Crl and σ^S during growth of *Salmonella* strains in LB0 at 28°C. ATCC 14028 (▲), ATCC*crl* (○), and ATCC*rpoS* (□) were grown in LB0 at 28°C. Exponential-phase cultures (optical density at 600 nm [OD600], 0.5) of *Salmonella* were diluted in LB0 prewarmed at 28°C to prolong the exponential phase. Aliquots were removed at various times and analyzed by Western blotting with anti-Crl and anti-σ^S antibodies. Ten micrograms of total protein was loaded in each slot. The growth phase was determined by measuring the culture turbidity at an optical density of 600 nm.

was able to complement the *rpoS* mutant for development of the rdar morphotype (Fig. 2). However, the *crl* mutant containing pSTK4 was also able to develop a typical rdar morphotype (Fig. 2). Accordingly, pSTK4 was able to complement the *crl* mutation for *csgD*, *csgB*, and *adrA* expression (Fig. 7A). The levels of σ^S from pSTK4 were higher than the levels from the chromosomal copy of *rpoS* (Fig. 7B). This increase in RpoS expression may alleviate the need for Crl for expression of the genes involved in the rdar morphotype. In the late exponential growth phase, the level of *csgD* expression in the presence of pSTK4 was slightly lower in the *crl* strain than in the wild-type strain, suggesting that, even in the presence of high levels of σ^S, Crl may still contribute to σ^S activity when cells enter the stationary phase (Fig. 7A).

Crl protein activates in vitro transcription by Eσ^S from the *csgD* and *adrA* promoters. We constructed pQE*crl*, which expressed a recombinant Crl protein containing six histidine residues at its N terminus. In pQE*crl*, expression of the six-His-tagged protein is controlled by the IPTG-inducible promoter of pQE30. As expected, after induction with IPTG, high levels of a 17-kDa protein were produced in *E. coli* JM109 carrying pQE*crl* (Fig. 8B, lane 2). We determined whether the His_6-Crl protein was still active by introducing pQE30 and pQE*crl* into the wild-type and *crl* strains of *Salmonella*. These derivative strains were spread on LB0 containing CR and grown for 6

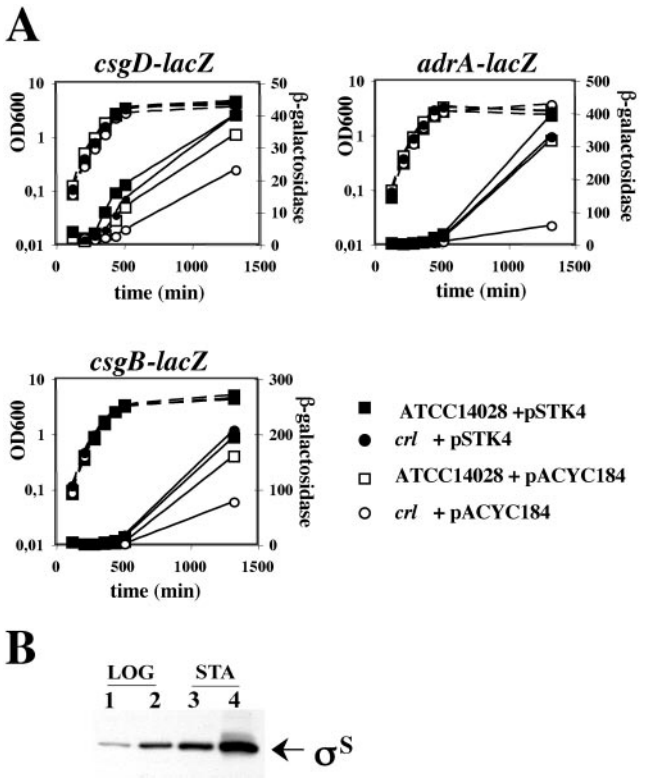

FIG. 7. Complementation of the *crl* mutation by the cloned *rpoS* gene. (A) Expression of *csgD-lacZ*, *adrA-lacZ*, and *csgB-lacZ* in the ATCC 14028 and ATCC*crl* strains containing the pACYC184 vector and the cloned *rpoS* gene on pSTK4. Exponential-phase cultures (optical density at 600 nm [OD600], 0.5) of *Salmonella* were diluted in LB0 prewarmed at 28°C to prolong the exponential phase. Aliquots were removed at various times, and β-galactosidase activity was measured (solid lines) by the method of Miller (29). The growth phase was determined by measuring the culture turbidity at an optical density of 600 nm (dashed lines). (B) RpoS production in the *Salmonella* cultures shown in panel A. Aliquots were removed during the exponential phase (LOG) (optical density at 600 nm = 0.4) and during the stationary phase (STA) (optical density at 600 nm = 2.5) of growth and were analyzed by Western blotting with anti-σ^S antibodies. Ten micrograms of total protein was loaded in each slot. Lanes 1 and 3, ATCC*csgD-lacZ* with the pACYC184 vector; lanes 2 and 4, ATCC*csgD-lacZ* with *rpoS* on pSTK4 (Table 1).

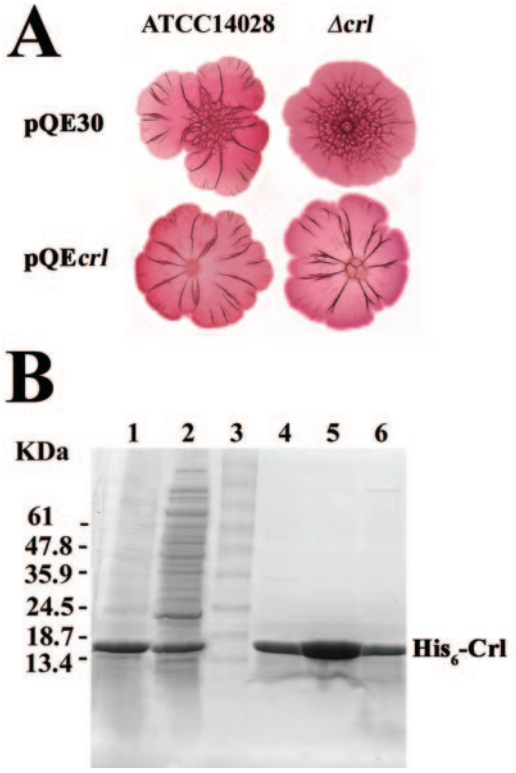

FIG. 8. In vivo activity and purification of the recombinant His_6-Crl protein. (A) Complementation of the *crl* mutant by His_6-Crl for expression of the rdar morphotype. ATCC 14028 and its Δ*crl* mutant derivative containing the pQE30 vector and pQE*crl* expressing the His_6-Crl protein were grown on CR plates for 6 days at 28°C. (B) Coomassie blue staining of 12% SDS–polyacrylamide gel. The overexpressed recombinant His_6-Crl protein was purified from JM109 carrying pQE*crl* using immobilized metal ion chromatography (lane 1) (see Materials and Methods). The protein was purified further on a Hitrap Q anion-exchange column. Fractions that eluted between 400 and 500 mM NaCl contained highly purified His_6-Crl (lanes 4 to 6). Lane 1, purified His_6-Crl protein on Ni-nitrilotriacetic acid resin (10 μg); lane 2, IPTG-induced JM109 extract containing pQE*crl* (10 μg); lane 3, molecular weight standards; lanes 4 to 6, purified His_6-Crl fractions eluted from the Hitrap Q anion-exchange column.

days at 28°C. The pQE*crl* plasmid was able to restore a typical rdar morphotype in the *crl* strain, whereas the pQE30 vector could not do this (Fig. 8A). This indicated that the His_6-Crl protein was active. The overexpressed recombinant protein was obtained from JM109 carrying pQE*crl* and was purified to homogeneity, as judged by electrophoresis in a denaturing polyacrylamide gel (Fig. 8B) and electrospray mass spectrometry (molecular weight, 17,195.4 ± 1.6). It was then used to produce polyclonal antibodies against Crl and in subsequent in vitro studies.

The in vivo studies showed that Crl played a role in the transcriptional activation of the σ^S-regulated genes *csgB*, *csgD*, *adrA*, and *bcsA*. We determined whether Crl played a direct role by carrying out in vitro transcription assays with the purified His_6-Crl protein. As the promoters for the *bcsABZC* operon have not been identified yet, we focused on the *csgB*, *csgD*, and *adrA* genes. We cloned the three promoters in front of transcriptional terminators (28). In preliminary experiments with *csgB*, no transcript of the expected size was observed with either $E\sigma^S$ or $E\sigma^{70}$. This was consistent with the results of Bougdour et al. (8), who suggested that an unknown factor that activates *csgB* expression, possibly the CsgD activator protein, was missing in the in vitro assay. By contrast, we observed significant levels of transcripts of the expected sizes in in vitro single-round runoff assays using the $E\sigma^S$ holoenzyme for the *csgD* promoter and for the *adrA* promoter (Fig. 9A). Addition of Crl increased the levels of transcripts initiating at the *csgD* and *adrA* promoters 1.5- and 2.5-fold, respectively, on linear templates (Fig. 9A, lanes 1 to 5). This showed that the Crl protein plays a direct role in transcription initiation by $E\sigma^S$ from the *csgD* and *adrA* promoters. We detected lower levels of *csgD* and *adrA* transcripts when $E\sigma^{70}$ was used instead of $E\sigma^S$ under the same conditions (Fig. 9A, lanes 6 and 7). This showed that σ^S plays a direct role in the transcription of *csgD* and *adrA*. However, Crl did not affect the efficiency of σ^{70}-dependent transcription at the *csgD* and *adrA* promoters and at

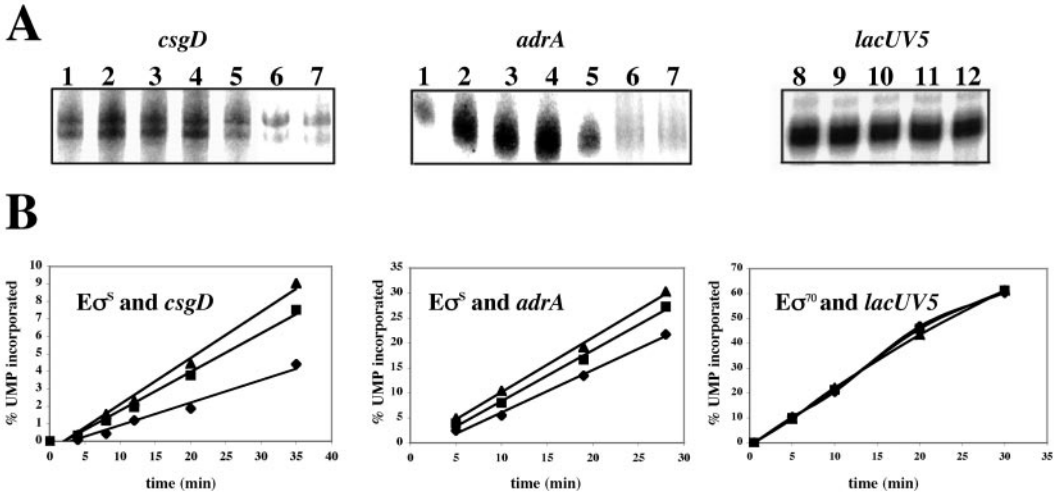

FIG. 9. In vitro transcription experiments. (A) Single-round in vitro transcription from the *csgD* and *adrA* promoters and the σ^{70}-dependent promoter *lac*UV5 by $E\sigma^S$ (lanes 1 to 5) and $E\sigma^{70}$ (lanes 6 to 12) with or without His_6-Crl. The holoenzyme was preincubated in the absence of His_6-Crl (lanes 1, 5, 6, 8, and 12) or in the presence of His_6-Crl (lanes 2 and 9, 250 nM; lanes 3 and 10, 1 μM; lanes 4, 7, and 11, 4 μM). Open complexes were then allowed to form by incubation at 30°C for 12 min before addition of heparin and XTPs. (B) Effect of His_6-Crl in kinetic abortive initiation assays. For *csgD* and *adrA*, $E\sigma^S$ was preincubated in the absence of His_6-Crl (◆) or in the presence of His_6-Crl (■, 250 nM; ▲, 1 μM). For *lac*UV5, $E\sigma^{70}$ was preincubated in the absence of His_6-Crl (◆) or in the presence of His_6-Crl (■, 250 nM; ▲, 1 μM). After addition of a mixture containing the promoter fragment, the dinucleotide initiator, and [α-^{32}P]UTP, the incorporation of labeled [α-^{32}P]UMP into small abortive transcripts was monitored as a function of time. ApG was used to initiate the synthesis of ApGpUpU at the *csgD* promoter. ApA was used to initiate the synthesis of ApApUpU at the *adrA* and *lac*UV5 promoters.

the σ^{70}-dependent *lac*UV5 promoter (Fig. 9A, lanes 6 to 12). Thus, transcriptional activation by Crl appeared to be specific for $E\sigma^S$.

Crl facilitates open complex formation by $E\sigma^S$ at the *csgD* and *adrA* promoters. We showed that Crl had a direct effect on open complex formation by performing kinetic abortive initiation experiments (Fig. 9B). This method does not require preincubation of a promoter and RNA polymerase and can directly and accurately monitor the rate of open complex formation. The *csgD* transcript starts with the sequence pppGp UpUpA, with an A at position −1 on the nontemplate strand (42). Therefore, we used the dinucleotide ApG and [α-^{32}P]UTP to obtain reiterative synthesis of ApG*pU*pU. The reaction was initiated by adding $E\sigma^S$ RNA polymerase to a mixture containing ApG, labeled UTP, and the *csgD* fragment, and we monitored the rate of tetranucleotide formation as a function of time (Fig. 9B). After a short lag time, the synthesis was linear up to 30 min. Crl at concentrations of 250 nM and 1 μM increased the amount of tetranucleotide synthesized 1.7-fold and 2-fold, respectively. We obtained similar results with the *adrA* promoter using ApA and [α-^{32}P]UTP to synthesize ApA*pU*pU from the template sequence (Fig. 9B). However, the Crl stimulation appeared to be less efficient than that observed in the runoff assays (Fig. 9A and B). We verified that the tetranucleotide synthesis was initiated from the promoters being studied by forming and probing open complexes for single-stranded thymines using $KMnO_4$ (Fig. 10). At the *adrA* promoter, $E\sigma^S$ formed a transcription bubble extending from position −8 to position 7 according to the transcription start determined from the homologous *E. coli yaiC* promoter (9). At the *csgD* promoter, the pattern of the single-stranded thymines appeared to be more extended, but the most reactive base

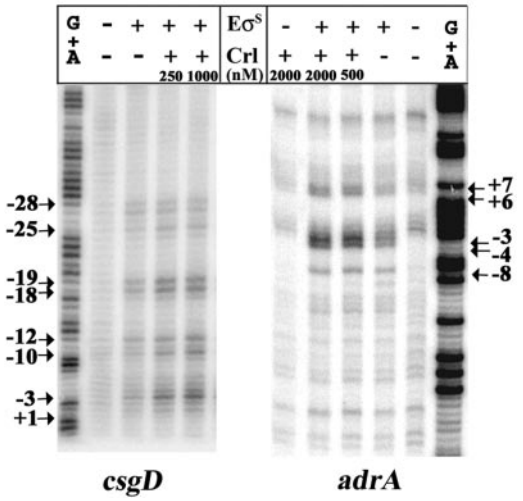

FIG. 10. $KMnO_4$ reactivity patterns of the *csgD* and *adrA* open complexes formed with and without His_6-Crl. After preincubation of $E\sigma^S$ with or without His_6-Crl at different concentrations, open complexes were allowed to form by incubation for 20 min at 30°C before the preparations were subjected to $KMnO_4$ attack. The positions of the reactive thymines were calibrated according to the G+A sequencing reaction and are indicated on the left for *csgD* (template strand) and on the right for *adrA* (nontemplate strand). The transcription start site of the *Salmonella csgDEFG* operon was determined previously (42), whereas the *adrA* start site was only tentatively assigned based on the homologous *E. coli yaiC* gene (9). Note that despite the conservation of the *adrA* and *yaiC* promoter sequences, the *adrA* start site might be shifted by a few nucleotides downstream from the start site of *yaiC*. Similar variation in the selection of start sites for *Salmonella* and *E. coli* genes was detected at *csgD* (42).

mapped at position −3, in agreement with the location of the transcription start site of the *Salmonella csgD* promoter (42). At each promoter, the reactivity of the transcription bubble thymines was clearly more intense in the presence of Crl, indicating that Crl had increased the amount of open complexes. Together, these results showed that Crl enhanced both the quantity of open complexes and the rate of formation of open complexes by $E\sigma^S$ from the *csgD* and *adrA* promoters. In contrast, Crl did not affect the rate of formation of open complexes by $E\sigma^{70}$ from the σ^{70}-dependent promoter *lac*UV5 (Fig. 9B).

DISCUSSION

We wanted to determine the physiological impact and the molecular function of Crl, a protein shown to bind σ^S and to enhance its activity. However, until now, there was no obvious phenotype associated with the *crl* mutant, although the protein has been identified as a regulator of curli biosynthesis in *E. coli*. It is noteworthy that the requirement for Crl seemed to vary from strain to strain (32, 37, 38). Curli production resulting in multicellular and aggregative behavior of the cells has been thoroughly investigated in different *S. enterica* serovars. At 28°C more than 90% of *Salmonella* serovar Typhimurium and Enteritidis strains develop the rdar morphotype, which is characterized by the formation of an extracellular matrix composed mainly of curli and cellulose (43). Single-cell behavior results from knockout of these two extracellular matrix components. Therefore, we decided to explore the effect of a *crl* null mutation on the rdar morphotype of *Salmonella* serovar Typhimurium.

The *crl* knockout mutant of *Salmonella* serovar Typhimurium strain ATCC 14028 was able to produce some curli and cellulose, but it developed an atypical rdar morphotype ($rdar_{crl}$) (Fig. 1). Scanning electron microscopy and transmission electron microscopy of wild-type colonies expressing the rdar morphotype and *crl* colonies expressing the $rdar_{crl}$ morphotype revealed different arrangements of the *crl* and wild-type cells in the extracellular matrix (Fig. 3). We also observed substantial differences in the quantity and organization of the extracellular matrix in thin sections stained with ruthenium red. Complementation of the *crl* mutation could be achieved with the cloned *crl* gene in pAC*crl*-1, confirming that Crl has a role in the development of the rdar morphotype (Fig. 2).

At the molecular level, the *crl* mutation decreased expression of *lacZ* gene fusions in the curli and the cellulose biosynthesis genes *csgD*, *csgB*, *adrA*, and *bcsA* (Fig. 5). CsgD depends on RpoS and Crl and controls the expression of *csgBAC* and *adrA* but not the expression of *bscA*. This indicates that at least two σ^S-regulated genes implicated in the formation of the rdar morphotype in *Salmonella* are affected by *crl*. The *crl* null allele effects were not as severe as the effects conferred by an *rpoS* null mutation. The effects caused by the *rpoS* mutation alone and the *rpoS crl* double mutation were similar, and we were not able to obtain complementation of the *crl* mutation with the cloned *crl* gene in the absence of RpoS (data not shown). Also, expression of Crl from pAC*crl*-1 did not modify the "saw" morphotype of the *rpoS* mutant (Fig. 2). Together, these results indicate that Crl function requires RpoS. Since the level of the RpoS protein did not decrease in the *crl* null strain but rather increased (Fig. 6) (see below), Crl appears to function together with RpoS, as previously suggested (35).

In vitro studies with purified His_6-Crl confirmed this conclusion by demonstrating that Crl has a direct role in σ^S-dependent transcription initiation at the *csgD* and *adrA* promoters (Fig. 9 and 10). In these experiments, we found no noticeable effect of the Crl protein on the basal level of σ^{70}-dependent expression of *adrA* and *csgD* and on the σ^{70}-dependent expression of *lac*UV5. This suggests that Crl-mediated activation is specific for σ^S-dependent transcription. $KMnO_4$ reactivity experiments and abortive initiation assays clearly showed that Crl activates $E\sigma^S$-dependent transcription by enhancing the rate of open complex formation. However, Crl is not a classical transcription factor since it does not bind DNA (35). In contrast, it associates with σ^S and likely also with the $E\sigma^S$ holoenzyme (8), which allows it to form open complexes more efficiently. Several mechanisms could explain Crl activation of σ^S-dependent promoters. σ^S has been shown to bind core in vitro with the weakest affinity among the seven sigma factors of *Enterobacteriacae* (26). Consistent with the model of sigma factor competition for a limited amount of core available in the cell, Crl could facilitate association of σ^S with the core enzyme. However, according to the study of Bougdour et al. (8) and our preliminary data, Crl does not play a role in the competition between σ^S and σ^{70} for core binding. Therefore, Crl should stimulate $E\sigma^S$ recruitment to the promoter. Further assays are needed to determine whether Crl facilitates closed complex formation, helps promoter opening, or affects both mechanisms. Also, our experiments do not exclude the possibility that Crl has additional effects at other steps of the transcription process (for example, facilitating promoter escape by the $E\sigma^S$ RNA polymerase). The apparently more efficient stimulation of transcription at the *adrA* promoter in single-round runoff experiments than in abortive initiation assays supports this idea. Like many transcription factors, Crl may affect different steps of transcription initiation at different promoters in a nonexclusive manner.

However, both in the absence and in the presence of the Crl protein we were unable to obtain noticeable in vitro transcription from the *csgB* promoter. This result, which is consistent with the results of Bougdour et al. (8), may have been due to the lack of the CsgD protein in the purified system. Indeed, it has been suggested, although it has never been shown, that CsgD binds to conserved 11-bp sequences upstream of the *csgB* and *adrA* promoters, activating transcription of these genes (9, 16). Unlike the *csgB* promoter, the *adrA* promoter does not necessarily require CsgD since in vitro transcription of *adrA* was successfully obtained in the absence of CsgD (Fig. 9). Until now, it was not known whether the role of RpoS at *adrA* and *csgBAC* is uniquely mediated through *csgD* or whether RpoS also plays a direct role in transcription initiation at these promoters. The *rpoS* mutation affected *adrA* and *csgB* expression more than a mutation in *csgD* affected this expression (Fig. 5B). This suggests that, in addition to positively regulating *csgD* expression, *rpoS* is also required at some other steps in *adrA* and *csgB* gene expression regulation. The results of our in vitro experiments support the hypothesis that σ^S has a direct role, at least at the *adrA* promoter. However, this does not exclude the possibility that $E\sigma^{70}$ has an additional role in transcription initiation at the *adrA* and *csgB* promoters, and we were able to

detect in vitro transcripts by $E\sigma^{70}$ from *adrA* and also from *csgD* (Fig. 9). Experiments with purified CsgD are needed to determine whether CsgD can activate transcription by $E\sigma^{S}$ and/or $E\sigma^{70}$ at the *adrA* and *csgB* promoters.

In agreement with the study of Zogaj et al. (58), we found that a *csgD* null mutation did not decrease the expression of the cellulose biosynthetic gene *bcsA* (Fig. 5A). However, the *rpoS* mutation affected the transcription of a *bcsA-lacZ* gene fusion (Fig. 5A). This indicates that at least two genes involved in cellulose biosynthesis are affected by RpoS, the CsgD-dependent gene *adrA* and the *bcsA* gene, whose expression is independent of CsgD. In agreement with this, we found that *adrA* on a plasmid was able to restore calcofluor binding to the *adrA* and *csgD* mutant strains but not to the *rpoS* and *bcsA* strains (data not shown). We did not expect regulation of *bcsA* by RpoS, as Zogaj et al. (58) found that a *bcsA-lacZ* gene fusion (we used the same gene fusion [Table 1]) was indeed partially induced in the stationary phase, but in an RpoS-independent manner. So far, we do not know the reason for this discrepancy. The strain used by Zogaj et al. (58) was a Nal^r derivative of ATCC 14028. It is possible that the Nal^r mutation interferes with expression of the *bcs* genes. Further experiments are needed to investigate the regulatory cues of the cellulose biosynthetic genes and their dependence on σ^S.

The interplay between *Salmonella* Crl and σ^S level and activity appears to be intricate. On the one hand, Crl binds to σ^S, directly increasing its efficiency in transcription initiation both in vivo and in vitro, and as expected, a *crl* null mutation can be complemented by an increase in RpoS expression (Fig. 2 and 7). On the other hand, the absence of a functional *crl* gene results in accumulation of increased levels of σ^S in *Salmonella* (Fig. 6), as previously shown for *E. coli* (8, 35). How can these two observations be reconciled?

The former result is fully consistent with the hypothesis that Crl promotes the recruitment of $E\sigma^S$ to the σ^S-dependent promoters, as we would expect an increase in RpoS levels to alleviate the need for Crl. It also seems to be in agreement with the previous finding for *E. coli* that the requirement of Crl for curli production is different in different strains (31, 32, 37, 38). This difference might be due to σ^S levels and activities that vary from one strain to another (22, 31, 35). It is likely that the requirement for Crl is more acute in cells expressing low levels of σ^S. The curli-deficient phenotype of strain HB101 is suppressed by either *crl* (32) or *rpoS* (31) on a plasmid. When present in HB101, *crl* may increase an otherwise low level of RpoS activity, and the increase would then be sufficient for curli production (35).

Altogether, our observations suggest that there is feedback control for Crl-dependent regulation of σ^S activity. For example, when Crl is missing and σ^S activity decreases, an increase in σ^S levels due to a lack of Crl may have a compensatory role. This phenomenon is reminiscent of the autoregulatory loop for the intracellular concentrations of σ^S and its anti-sigma factor, RssB, in *E coli* (for a review see reference 19). Phosphorylated RssB that binds σ^S negatively controls σ^S levels through ClpXP degradation. This in turn decreases *rssB* transcription from its σ^S-dependent promoter, leading to a decrease in the RssB level and consequently to an increase in the σ^S level. It remains to be determined whether Crl is involved in this autoregulatory control by directly stimulating *rssB* transcription.

ACKNOWLEDGMENTS

We thank Ute Römling for providing bacterial strains and Ulrich Gerstel for constructing plasmid pU-2750.

This work was supported by research funds from the Pasteur Institut and CNRS.

REFERENCES

1. **Arnqvist, A., A. Olsen, J. Pfeifer, D. G. Russell, and S. Normark.** 1992. The Crl protein activates cryptic genes for curli formation and fibronectin binding in *Escherichia coli* HB101. Mol. Microbiol. **6:**2443–2452.
2. **Austin, J. W., G. Sanders, W. W. Kay, and S. K. Collinson.** 1998. Thin aggregative fimbriae enhance *Salmonella enteritidis* biofilm formation. FEMS Microbiol. Lett. **162:**295–301.
3. **Barak, J. D., L. Gorski, P. Naraghi-Arani, and A. O. Charkowski.** 2005. *Salmonella enterica* virulence genes are required for bacterial attachment to plant tissue. Appl. Environ. Microbiol. **71:**5685–5691.
4. **Ben Nasr, A., A. Olsen, U. Sjöbring, W. Müller-Esterl, and L. Björck.** 1996. Assembly of human contact phase proteins and release of bradykinin at the surface of curli-expressing *Escherichia coli*. Mol. Microbiol. **20:**927–935.
5. **Bian, Z., A. Brauner, Y. Li, and S. Normark.** 2000. Expression of and cytokine activation by *Escherichia coli* curli fibers in human sepsis. J. Infect. Dis. **181:**602–612.
6. **Bian, Z., Z. Q. Yan, G. K. Hansson, P. Thoren, and S. Normark.** 2001. Activation of inducible nitric oxide synthase/nitric oxide by curli fibers leads to a fall in blood pressure during systemic *Escherichia coli* infection in mice. J. Infect. Dis. **183:**612–619.
7. **Bokranz, W., X. Wang, H. Tschape, and U. Romling.** 2005. Expression of cellulose and curli fimbriae by *Escherichia coli* isolated from the gastrointestinal tract. J. Med. Microbiol. **54:**1171–1182.
8. **Bougdour, A., C. Lelong, and J. Geiselmann.** 2004. Crl, a low temperature-induced protein in *Escherichia coli* that binds directly to the stationary phase sigma subunit of RNA polymerase. J. Biol. Chem. **279:**19540–19550.
9. **Brombacher, E., C. Dorel, A. J. Zehnder, and P. Landini.** 2003. The curli biosynthesis regulator CsgD co-ordinates the expression of both positive and negative determinants for biofilm formation in *Escherichia coli*. Microbiology **149:**2847–2857.
10. **Chang, A. C., and S. N. Cohen.** 1978. Construction and characterization of amplifiable multicopy DNA cloning vehicles derived from the P15A cryptic miniplasmid. J. Bacteriol. **134:**1141–1156.
11. **Collinson, S. K., S. C. Clouthier, J. L. Doran, P. A. Banser, and W. W. Kay.** 1996. *Salmonella enteritidis agfBAC* operon encoding thin, aggregative fimbriae. J. Bacteriol. **178:**662–667.
12. **Coynault, C., V. Robbe-Saule, and F. Norel.** 1996. Virulence and vaccine potential of *Salmonella typhimurium* mutants deficient in the expression of the RpoS (sigma S) regulon. Mol. Microbiol. **22:**149–160.
13. **Datsenko, K. A., and B. L. Wanner.** 2000. One-step inactivation of chromosomal genes in *Escherichia coli* K-12 using PCR products. Proc. Natl. Acad. Sci. USA **97:**6640–6645.
14. **Dibb-Fuller, M. P., E. Allen-Vercoe, C. J. Thorns, and M. J. Woodward.** 1999. Fimbriae- and flagella-mediated association with and invasion of cultured epithelial cells by *Salmonella enteritidis*. Microbiology **145:**1023–1031.
15. **Ellermeier, C. D., A. Janakiraman, and J. M. Slauch.** 2002. Construction of targeted single copy lac fusions using lambda Red and FLP-mediated site-specific recombination in bacteria. Gene **290:**153–161.
16. **Gerstel, U., and U. Römling.** 2003. The *csgD* promoter, a control unit for biofilm formation in *Salmonella typhimurium*. Res. Microbiol. **154:**659–667.
17. **Gophna, U., M. Barlev, R. Seijffers, T. A. Oelschlager, J. Hacker, and E. Z. Ron.** 2001. Curli fibers mediate internalization of *Escherichia coli* by eukaryotic cells. Infect. Immun. **69:**2659–2665.
18. **Hammar, M., A. Arnqvist, Z. Bian, A. Olsen, and S. Normark.** 1995. Expression of two *csg* operons is required for production of fibronectin- and Congo red-binding curli polymers in *Escherichia coli* K-12. Mol. Microbiol. **18:**661–670.
19. **Hengge-Aronis, R.** 2002. Signal transduction and regulatory mechanisms involved in control of the sigma(S) (RpoS) subunit of RNA polymerase. Microbiol. Mol. Biol. Rev. **66:**373–395.
20. **Herwald, H., M. Mörgelin, A. Olsen, M. Rhen, B. Dahlbäck, W. Müller-Esterl, and L. Björck.** 1998. Activation of the contact-phase system on bacterial surfaces—a clue to serious complications in infectious diseases. Nat. Med. **4:**298–302.
21. **Ishihama, A.** 2000. Functional modulation of *Escherichia coli* RNA polymerase. Annu. Rev. Microbiol. **54:**499–518.
22. **King, T., A. Ishihama, A. Kori, and T. Ferenci.** 2004. A regulatory trade-off as a source of strain variation in the species *Escherichia coli*. J. Bacteriol. **186:**5614–5620.
23. **Kowarz, L., C. Coynault, V. Robbe-Saule, and F. Norel.** 1994. The *Salmonella typhimurium katF* (*rpoS*) gene: cloning, nucleotide sequence, and regulation of *spvR* and *spvABCD* virulence plasmid genes. J. Bacteriol. **176:**6852–6860.
24. **La Ragione, R. M., W. A. Cooley, and M. J. Woodward.** 2000. The role of fimbriae and flagella in the adherence of avian strains of *Escherichia coli*

O78:K80 to tissue culture cells and tracheal and gut explants. J. Med. Microbiol. **49:**327–338.
25. **Luft, J. H.** 1971. Ruthenium red and violet. I. Chemistry, purification, methods of use for electron microscopy and mechanism of action. Anat. Rec. **171:**347–368.
26. **Maeda, H., N. Fujita, and A. Ishihama.** 2000. Competition among seven *Escherichia coli* sigma subunits: relative binding affinities to the core RNA polymerase. Nucleic Acids Res. **28:**3497–3503.
27. **Malan, T. P., A. Kolb, H. Buc, and W. R. McClure.** 1984. Mechanism of CRP-cAMP activation of *lac* operon transcription initiation activation of the P1 promoter. J. Mol. Biol. **180:**881–909.
28. **Marschall, C., V. Labrousse, M. Kreimer, D. Weichart, A. Kolb, and R. Hengge-Aronis.** 1998. Molecular analysis of the regulation of *csiD*, a carbon starvation-inducible gene in *Escherichia coli* that is exclusively dependent on sigmaS and requires activation by cAMP-CRP. J. Mol. Biol. **276:**339–353.
29. **Miller, J. H.** 1972. Experiments in molecular genetics. Cold Spring Harbor Laboratory, Cold Spring Harbor, N.Y.
30. **Olsen, A., A. Arnqvist, M. Hammar, and S. Normark.** 1994. Environmental regulation of curli production in *Escherichia coli*. Infect. Agents Dis. **2:**272–274.
31. **Olsen, A., A. Arnqvist, M. Hammar, S. Sukupolvi, and S. Normark.** 1993. The RpoS sigma factor relieves H-NS-mediated transcriptional repression of *csgA*, the subunit gene of fibronectin-binding curli in *Escherichia coli*. Mol. Microbiol. **7:**523–536.
32. **Olsen, A., A. Jonsson, and S. Normark.** 1989. Fibronectin binding mediated by a novel class of surface organelles on *Escherichia coli*. Nature **338:**652–655.
33. **Olsen, A., M. J. Wick, M. Mörgelin, and L. Björck.** 1998. Curli, fibrous surface proteins of *Escherichia coli*, interact with major histocompatibility complex class I molecules. Infect. Immun. **66:**944–949.
34. **Orsini, G., A. Kolb, and H. Buc.** 2001. The *Escherichia coli* RNA polymerase anti-sigma 70 AsiA complex utilizes alpha-carboxyl-terminal domain upstream promoter contacts to transcribe from a −10/−35 promoter. J. Biol. Chem. **276:**19812–19819.
35. **Pratt, L. A., and T. J. Silhavy.** 1998. Crl stimulates RpoS activity during stationary phase. Mol. Microbiol. **29:**1225–1236.
36. **Prigent-Combaret, C., G. Prensier, T. T. Le Thi, O. Vidal, P. Lejeune, and C. Dorel.** 2000. Developmental pathway for biofilm formation in curli-producing *Escherichia coli* strains: role of flagella, curli and colanic acid. Environ. Microbiol. **2:**450–464.
37. **Provence, D. L., and R. Curtiss III.** 1994. Isolation and characterization of a gene involved in hemagglutination by an avian pathogenic *Escherichia coli* strain. Infect. Immun. **62:**1369–1380.
38. **Provence, D. L., and R. Curtiss III.** 1992. Role of *crl* in avian pathogenic *Escherichia coli*: a knockout mutation of *crl* does not affect hemagglutination activity, fibronectin binding, or curli production. Infect. Immun. **60:**4460–4467.
39. **Robbe-Saule, V., F. Schaeffer, L. Kowarz, and F. Norel.** 1997. Relationships between H-NS, sigma S, SpvR and growth phase in the control of *spvR*, the regulatory gene of the *Salmonella* plasmid virulence operon. Mol. Gen. Genet. **256:**333–347.
40. **Römling, U.** 2005. Characterization of the rdar morphotype, a multicellular behaviour in *Enterobacteriaceae*. Cell. Mol. Life Sci. **62:**1234–1246.
41. **Römling, U.** 2001. Genetic and phenotypic analysis of multicellular behavior in *Salmonella typhimurium*. Methods Enzymol. **336:**48–59.
42. **Römling, U., Z. Bian, M. Hammar, W. D. Sierralta, and S. Normark.** 1998. Curli fibers are highly conserved between *Salmonella typhimurium* and *Escherichia coli* with respect to operon structure and regulation. J. Bacteriol. **180:**722–731.
43. **Römling, U., W. Bokranz, W. Rabsch, X. Zogaj, M. Nimtz, and H. Tschäpe.** 2003. Occurrence and regulation of the multicellular morphotype in *Salmonella* serovars important in human disease. Int. J. Med. Microbiol. **293:**273–285.
44. **Römling, U., and M. Rohde.** 1999. Flagella modulate the multicellular behavior of *Salmonella typhimurium* on the community level. FEMS Microbiol. Lett. **180:**91–102.
45. **Romling, U., M. Rohde, A. Olsen, S. Normark, and J. Reinköster.** 2000. AgfD, the checkpoint of multicellular and aggregative behaviour in *Salmonella typhimurium* regulates at least two independent pathways. Mol. Microbiol. **36:**10–23.
46. **Römling, U., W. D. Sierralta, K. Eriksson, and S. Normark.** 1998. Multicellular and aggregative behaviour of *Salmonella typhimurium* strains is controlled by mutations in the *agfD* promoter. Mol. Microbiol. **28:**249–264.
47. **Ryu, J. H., and L. R. Beuchat.** 2005. Biofilm formation by *Escherichia coli* O157:H7 on stainless steel: effect of exopolysaccharide and curli production on its resistance to chlorine. Appl. Environ. Microbiol. **71:**247–254.
48. **Sambrook, J., E. F. Fritsch, and T. Maniatis.** 1989. Molecular cloning: a laboratory manual, 2nd ed. Cold Spring Harbor Laboratory, Cold Spring Harbor, N.Y.
49. **Schmieger, H.** 1972. Phage P22-mutants with increased or decreased transduction abilities. Mol. Gen. Genet. **119:**75–88.
50. **Silhavy, T. J., M. L. Bernman, and L. W. Ernqvist.** 1984. Experiments with gene fusions. Cold Spring Harbor Laboratory, Cold Spring Harbor, N.Y.
51. **Sjöbring, U., G. Pohl, and A. Olsen.** 1994. Plasminogen, absorbed by *Escherichia coli* expressing curli or by *Salmonella enteritidis* expressing thin aggregative fimbriae, can be activated by simultaneously captured tissue-type plasminogen activator (t-PA). Mol. Microbiol. **14:**443–452.
52. **Solano, C., B. Garcia, J. Valle, C. Berasain, J. M. Ghigo, C. Gamazo, and I. Lasa.** 2002. Genetic analysis of *Salmonella enteritidis* biofilm formation: critical role of cellulose. Mol. Microbiol. **43:**793–808.
53. **Sternberg, N. L., and R. Maurer.** 1991. Bacteriophage-mediated generalized transduction in *Escherichia coli* and *Salmonella typhimurium*. Methods Enzymol. **204:**18–43.
54. **Sukupolvi, S., R. G. Lorenz, J. I. Gordon, Z. Bian, J. D. Pfeifer, S. J. Normark, and M. Rhen.** 1997. Expression of thin aggregative fimbriae promotes interaction of *Salmonella typhimurium* SR-11 with mouse small intestinal epithelial cells. Infect. Immun. **65:**5320–5325.
55. **Tükel, C., M. Raffatellu, A. D. Humphries, R. P. Wilson, H. L. Andrews-Polymenis, T. Gull, J. F. Figueiredo, M. H. Wong, K. S. Michelsen, M. Akcelik, L. G. Adams, and A. J. Bäumler.** 2005. CsgA is a pathogen-associated molecular pattern of *Salmonella enterica* serotype Typhimurium that is recognized by Toll-like receptor 2. Mol. Microbiol. **58:**289–304.
56. **Van der Velden, A. W., A. J. Baumler, R. M. Tsolis, and F. Heffron.** 1998. Multiple fimbrial adhesins are required for full virulence of *Salmonella typhimurium* in mice. Infect. Immun. **66:**2803–2808.
57. **Woodward, M. J., M. Sojka, K. A. Sprigings, and T. J. Humphrey.** 2000. The role of SEF14 and SEF17 fimbriae in the adherence of *Salmonella enterica* serotype Enteritidis to inanimate surfaces. J. Med. Microbiol. **49:**481–487.
58. **Zogaj, X., M. Nimtz, M. Rohde, W. Bokranz, and U. Römling.** 2001. The multicellular morphotypes of *Salmonella typhimurium* and *Escherichia coli* produce cellulose as the second component of the extracellular matrix. Mol. Microbiol. **39:**1452–1463.